Conference Proceedings of the Society for Experimental Mechanics Series

Nancy Sottos · Robert Rowlands
Kathryn Dannemann *Editors*

Experimental and Applied Mechanics, Volume 6

Proceedings of the 2014 Annual Conference on Experimental and Applied Mechanics

SEM

Springer

Nancy Sottos • Robert Rowlands • Kathryn Dannemann
Editors

Experimental and Applied Mechanics, Volume 6

Proceedings of the 2014 Annual Conference on Experimental and Applied Mechanics

Springer

Editors
Nancy Sottos
Beckman Institute
University of Illinois
Urbana-Champaign
Urbana, IL, USA

Kathryn Dannemann
Southwest Research Institute
San Antonio, TX, USA

Robert Rowlands
University of Wisconsin
Madison, WI, USA

ISSN 2191-5644
ISBN 978-3-319-06988-3
DOI 10.1007/978-3-319-06989-0
Springer Cham Heidelberg New York Dordrecht London

ISSN 2191-5652 (electronic)
ISBN 978-3-319-06989-0 (eBook)

Library of Congress Control Number: 2011928691

Printed on acid-free paper

Springer is part of Springer Science+Business Media (www.springer.com)

Conference Proceedings of the Society for Experimental Mechanics Series

Series Editor
Tom Proulx
Society for Experimental Mechanics, Inc.
Bethel, CT, USA

For further volumes:
http://www.springer.com/series/8922

Preface

Experimental and Applied Mechanics, Volume 6: Proceedings of the 2014 Annual Conference on Experimental and Applied Mechanics represents one of eight volumes of technical papers presented at the 2014 SEM Annual Conference & Exposition on Experimental and Applied Mechanics organized by the Society for Experimental Mechanics and held in Greenville, SC, June 2–5, 2014. The complete Proceedings also includes volumes on: *Dynamic Behavior of Materials*; *Challenges in Mechanics of Time-Dependent Materials*; *Advancement of Optical Methods in Experimental Mechanics*; *Mechanics of Biological Systems and Materials*; *MEMS and Nanotechnology*; *Experimental Mechanics of Composite, Hybrid, and Multifunctional Materials*; *Fracture, Fatigue, Failure and Damage Evolution*.

Each collection presents early findings from experimental and computational investigations of an important topic within the field of Experimental Mechanics. This volume includes papers on Residual Stress, Thermomechanics and Infrared Imaging, Hybrid Techniques and Inverse Problems.

Residual stresses are especially important in engineering systems and design. The insidious nature of residual stresses often causes them to be underrated or overlooked. However, they profoundly influence structural design and substantially affect strength, fatigue life, and dimensional stability. Since residual stresses are induced during most materials processing procedures, for example, welding/joining, casting, thermal conditioning, and forming, they must be included and addressed in engineering design and applications.

In recent years the applications of infrared imaging techniques to the mechanics of materials and structures have grown considerably. The expansion is marked by the increased spatial and temporal resolution of the infrared detectors, faster processing times, and much greater temperature resolution. The improved sensitivity and more reliable temperature calibrations of the devices have meant that more accurate data can be obtained than were previously available.

Advances in inverse identification techniques have been coupled with optical methods that provide surface deformation measurements and volumetric measurements of materials. In particular, inverse methodology was developed to more fully use the dense spatial data provided by optical methods to identify mechanical constitutive parameters of materials. Since its beginnings during the 1980s, creativity in inverse methods has led to applications for a wide range of materials, with different constitutive behavior, across heterogeneous material interfaces. Complex test fixtures have been implemented to produce the necessary strain fields for identification. Force reconstruction has been developed for high strain rate testing. As developments in optical methods improve for both very large and very small length scales, applications of inverse identification methods have expanded to include geological and atomistic events.

Urbana, IL, USA — Nancy Sottos
Madison, WI, USA — Robert Rowlands
San Antonio, TX, USA — Kathryn Dannemann

Contents

Chapter 1
Electrical Impedance Spectroscopy for Structural Health Monitoring

Geoffrey A. Slipher, Robert A. Haynes, and Jaret C. Riddick

Abstract Structural heath monitoring (SHM) can provide an estimate of the state of damage in a structure, and of the remaining useful life of that structure. The work presented here is an investigation of a proposed new SHM technique for composite structures composed of carbon-fiber-reinforced-polymers (CFRP). Electrical impedance spectroscopy (EIS) is employed to estimate the damage state of the composite. No modification to current CFRP processing methods is required, nor is the proposed technique invasive or destructive. EIS interfaces can be either permanently attached or temporarily connected. We hypothesize that EIS has the potential to be more sensitive and selective for damage detection by using a full complex-plane analysis, considering both impedance magnitude and phase angle. This is in contrast to electrical SHM approaches employing resistance measurement, the real component of impedance, which ignores phase angle and reactance information. In order to test our hypothesis we implemented three different experiments to evaluate the effectiveness of the EIS technique: (1) specimen load sensitivity; (2) specimen damage sensitivity; and (3) specimen fatigue sensitivity. Multiple electrical interrogation paths through the specimen are considered.

Keywords Electrical impedance spectroscopy • Structural health monitoring • Carbon fiber • Fatigue state • Damage state detection • Load state detection

1.1 Introduction

Carbon-fiber reinforced composite materials are rapidly gaining wide use for a variety of applications pertaining to aircraft, spacecraft and civil infrastructure. The recent trend toward condition-based maintenance of advanced structural platforms has given rise to sensor-based monitoring of critical structural components. Structural health monitoring refers to the use of sensor data as a means to provide an estimate of the state of damage in a structure, and of the remaining useful life of that structure. Pervasive use of SHM in composite structures in the future will enable new structural applications that exploit the presence of sensors to enable novel lightweight designs and reduced maintenance burdens.

Damage detection by structural self-sensing in carbon fiber composites has been investigated thoroughly in the literature. In particular concepts for the use of electrical resistance measurements to detect damage in fiber-reinforced composites have been investigated, showing that resistance changes irreversibly upon damage inflicted by flexure, tension, fatigue, and impact [1]. Resistance change can be associated with the mode of damage. For example, fiber breakage increases the longitudinal resistance, and delamination increases the through-thickness resistance. Embedding of carbon nanotubes (CNTs) into glass-epoxy composites to create percolating electrical networks for sensing damage has been shown to work based on measuring the change in resistance due to cracking [2–5].

Electrical resistance measurements have shown some promise in the detection of damage in fiber composites, particularly in those systems where embedded sensors or electrical networks were used. However, electrical impedance measurements have the potential to be more sensitive and selective for damage detection by using a full complex-plane analysis, considering both impedance magnitude and phase angle. Electrical resistance can be considered zero-phase angle impedance. Impedance-based methods have been employed for qualitative health monitoring by correlating variations in mechanical impedance to

G.A. Slipher (✉) • R.A. Haynes • J.C. Riddick
Vehicle Technology Directorate, U.S. Army Research Laboratory, Aberdeen Proving Ground, MD 21005, USA
e-mail: geoffrey.a.slipher.civ@mail.mil

N. Sottos et al. (eds.), *Experimental and Applied Mechanics, Volume 6: Proceedings of the 2014 Annual Conference on Experimental and Applied Mechanics*, Conference Proceedings of the Society for Experimental Mechanics Series,
DOI 10.1007/978-3-319-06989-0_1,

electrical impedance measurements of a piezoelectric patch [6]. Experimental measurements of carbon fiber composites with embedded piezoceramic patches have shown a close connection between mechanical properties and impedance [7]. Electrical conductivity measurements of embedded CNT thin films have been used to detect damage from low velocity impacts in glass fiber reinforced polymer composites [8]. The electrical impedance tomography response of the composite with the electrical conductive strain sensitive embedded thin film was measured by recording current-voltage measurements at the periphery of the composite. More recent work has shown the effectiveness of using piezoelectric patches to monitor the health of adhesive joints in composites subjected to various environmental conditions using electro-mechanical impedance [9].

Other recent approaches that rely on impedance and frequency related responses have been presented in the literature. An approach for probing embedded sensors wirelessly using inductive coupling depends on electrical impedance, acoustic response, and pulse-echo response of the system [10]. Another study shows the promise of using metamaterial electromagnetic lenses to detect delaminations in composite materials by extracting effective magnetic permeability and frequency measurements [11].

Carbon fiber composites have been shown to be excellent electromagnetic interference (EMI) shielding materials with low surface impedance and high reflectivity [12]. Several models have been presented for electromagnetic characterization of fiber composites [13]. Models for effective properties of fiber composites commonly used in aircraft EMI shielding often employ various levels of detail, and therefore capture various physical aspects in the estimation values such as the reflection and transmission coefficients.

The approach of embedding conductive networks or sensor/actuator patches has proven to be effective in exploiting the electromechanical impedance of composite material systems. The work presented here employs electrical impedance spectroscopy (EIS) to estimate the damage state of the carbon fiber reinforced composites without the modifications introduced by embedding conductive networks or sensors. EIS interfaces can be either permanently attached or temporarily connected. Multiple interrogation paths through the specimen are considered. If successful, the present method would offer the potential of an inspection method for SHM that depends wholly on the intrinsic properties of the material. This paper contains a description of the composite material considered, along with a description of the experimental procedure.

1.2 Motivation

We are seeking structural health monitoring techniques that are simple and readily implementable, involve minimal modification to existing CFRP component manufacturing techniques, can operate in real-time, have minimal cost, and have the potential to spatially resolve damage and/or damage precursor locations. Our hypothesis that we are testing, in part with the methods described in this paper, is that by moving beyond resistance measurement techniques to EIS we can make a significant step toward achieving these objectives, in particular minimal cost and impact to existing manufacturing techniques. Electrical interrogation techniques, such as resistance or impedance measurement, require only simple electrical connection to an electrically conductive specimen, such as carbon fiber reinforced components. For this reason they are attractive as minimally invasive techniques that require little or no modification to the way carbon fiber components are manufactured. As damage is introduced to a carbon fiber reinforced component, electrical properties change, and that change can be detected and correlated with the type and location of the damage. Fiber breakage is expected to manifest predominantly as variations in component resistivity as well as in higher frequency response characteristics due to variations in the effective antenna length paths within a component. Delamination is expected to manifest predominantly as variations in the capacitive reactivity of the specimen as the physical spacing between parallel layers varies. A method with the capability to simultaneously detect changes in resistivity, frequency response, and reactivity would thus be required to resolve as many damage modes as possible. Resistance measurement techniques provide only one dimension of information along the real axis of the complex plane to resolve damage in CFRP components. Impedance analysis techniques add two additional dimensions of information: reactance and phase, as shown in Fig. 1.1. We therefore propose the EIS method as a potential improvement in NDE methods for CFRP structural health monitoring in Army systems such as rotorcraft. This paper describes initial experimental efforts to validate these hypotheses.

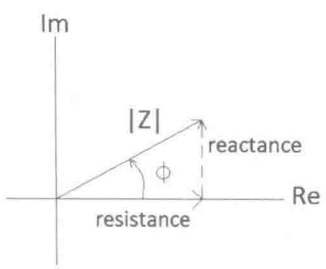

Fig. 1.1 Impedance complex plane

1.3 Experimental Procedure

Fifteen specimens were manufactured from a woven graphite/epoxy material system with a thickness of 0.125 in. and cut to dimensions of 1 in. by 12 in. Tabs of dimension 1.25 in. by 3 in. were attached to both sides and both ends of the specimen. The tabs extended 0.125 in. beyond the specimen on both sides and the end to reduce the likelihood that the wire leads would touch the testing machine; see Fig. 1.2. Five of the specimens were used to estimate the material's static strength as 68 kN, five specimens were used to estimate the material's fatigue life, and five specimens underwent cyclic loading with predefined pauses to record impedance measurements.

The cyclic loading was performed in an MTS 22-kip load frame with an MTS FlexTest 40 controller. An R-ratio of 0.1 was used with a maximum load of 55 kN and a frequency of 5 Hz. Silver epoxy was used to attach wire leads to the specimen in the configuration shown in Fig. 1.2. Five different electrical paths were interrogated through the specimen: A1-B1, A2-B2, A3-B2, A4-B3, and A5-B3. Electrical impedance was measured using an Agilent E5061B-LF network analyzer (NA) using a port 1–2 thru series method. Prior to initiating sample characterization, a calibration procedure was executed on the NA that pushed the calibration plane out to the specimen. The A1-A5 connections were used to inject the electrical signal through port 1, and the B1-3 connections were connected to port 2 for the NA return. For the fatigue tests, cyclic loading was applied as described above. Cyclic loading was stopped periodically and logarithmic frequency scans were performed with the NA from 1 kHz to 100 MHz for both statically loaded (55 kN) and unloaded states through each of the five electrical paths. Impedance magnitude and phase angle data were collected and saved. The electrical interrogation signal was a sine wave of varying frequency with power of 10 dBm (707 mV @ 50 Ω). During the first sample run, a manual testing protocol for running the impedance scans was used, and was identified as undesirable for two key reasons: (1) it consumed too much personnel time; (2) it introduced error in the data in the form of jump discontinuities in the cycle/failure domain as shown in Fig. 1.3. We believe the discontinuities arose from small variations in the calibration introduced by shutting down the equipment at night and recalibrating in the morning.

For both of the above stated reasons an around-the-clock automated testing routine was developed and implemented for the subsequent four samples described in this paper. The key component of the automated testing routine was the switching electronics that used magnetic reed relays triggered by a custom-programmed IC to switch between each of the five conductive paths through the specimen. Implementation of the automated routine completely eliminated the jump discontinuities in the cycle/failure domain. The automated experimental setup is shown in Fig. 1.4.

1.4 Results and Discussion

In order to test our hypotheses outlined above we implemented three different experiments to evaluate the effectiveness of the EIS technique: (1) specimen load sensitivity; (2) specimen damage sensitivity; and (3) specimen fatigue sensitivity. The specimen load sensitivity experiment involved incrementing the load applied to the specimen to identify if the EIS technique could detect changes in load levels. The damage sensitivity experiment involved scanning an undamaged specimen and subsequently introducing gross damage to the gage length and rescanning to determine if the EIS technique could detect the damage. The fatigue sensitivity experiment involved scanning the specimen at various numbers of loading cycles to identify whether or not the EIS technique can detect fatigue-related damage or damage precursors. The results of these three experiments are presented and discussed below.

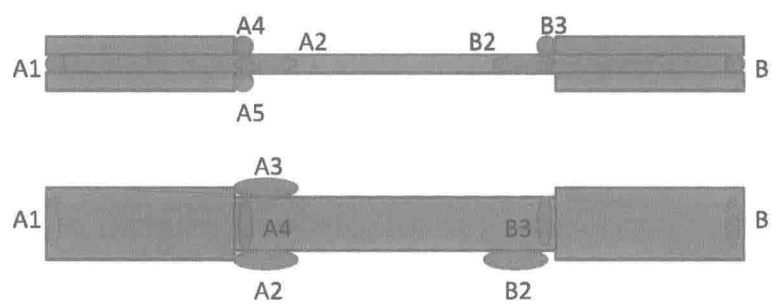

Fig. 1.2 Specimen configuration

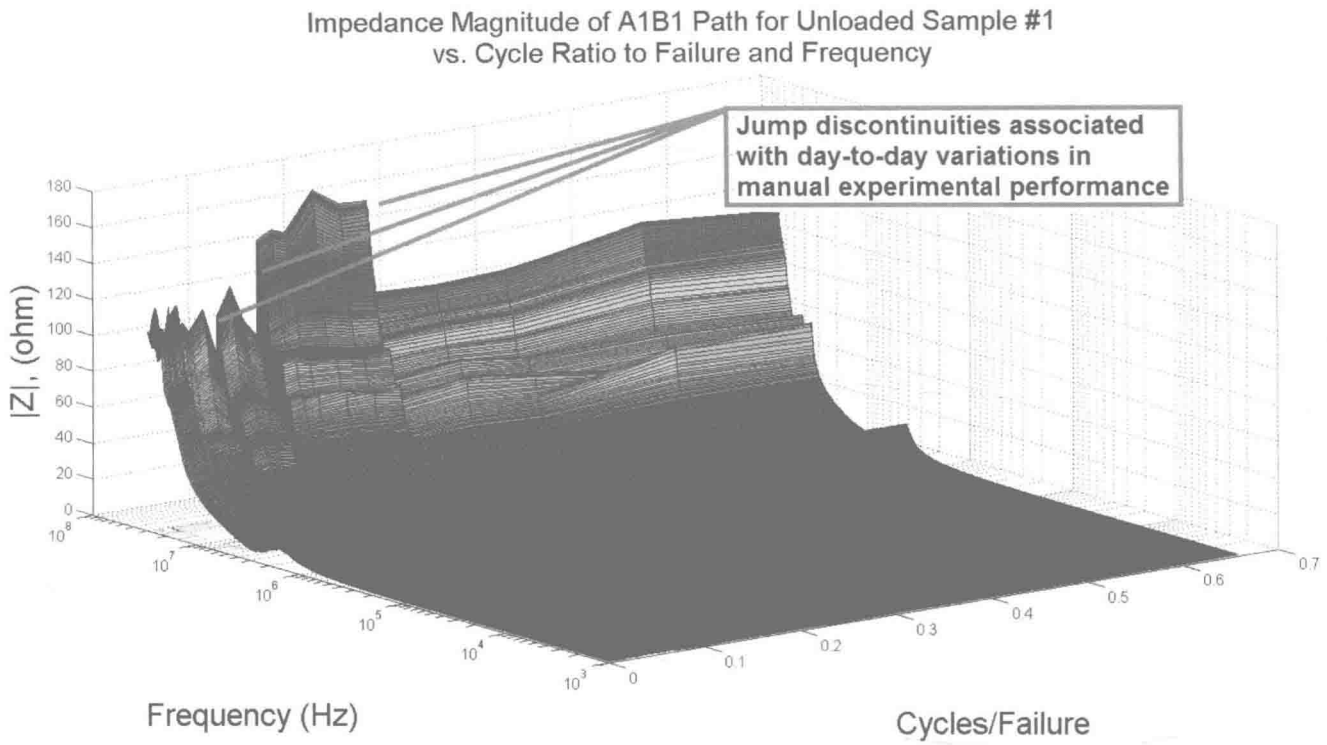

Fig. 1.3 Jump discontinuities in the data arising from manual data collection procedure, eliminated by implementing an automated procedure

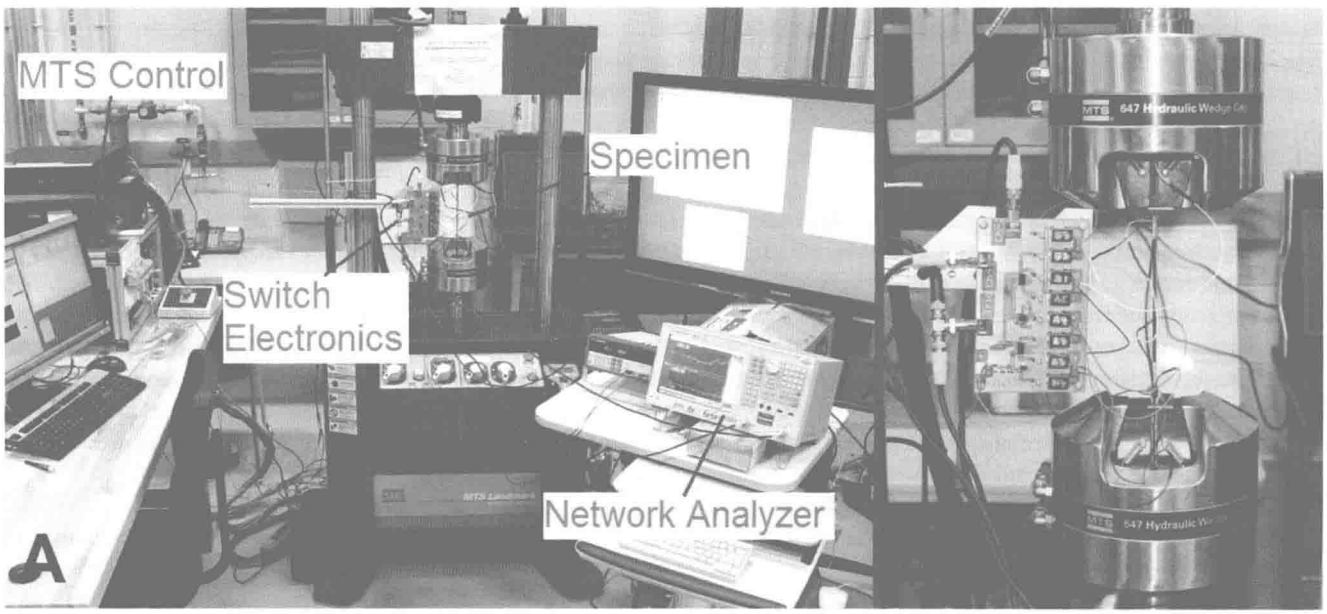

Fig. 1.4 Automated experimental setup: (**a**) wide view; (**b**) close-in specimen view with switching electronics

1.4.1 Detection of Specimen Load State

Load on specimen 'S6' was incremented from 0 to 50 kN, and all five electrical paths were interrogated using the NA at each load increment. The results for phase angle can be seen in Fig. 1.5 and impedance magnitude in Fig. 1.6. Specimen load resulting in strain can be detected using both impedance magnitude and phase information from the EIS scans.

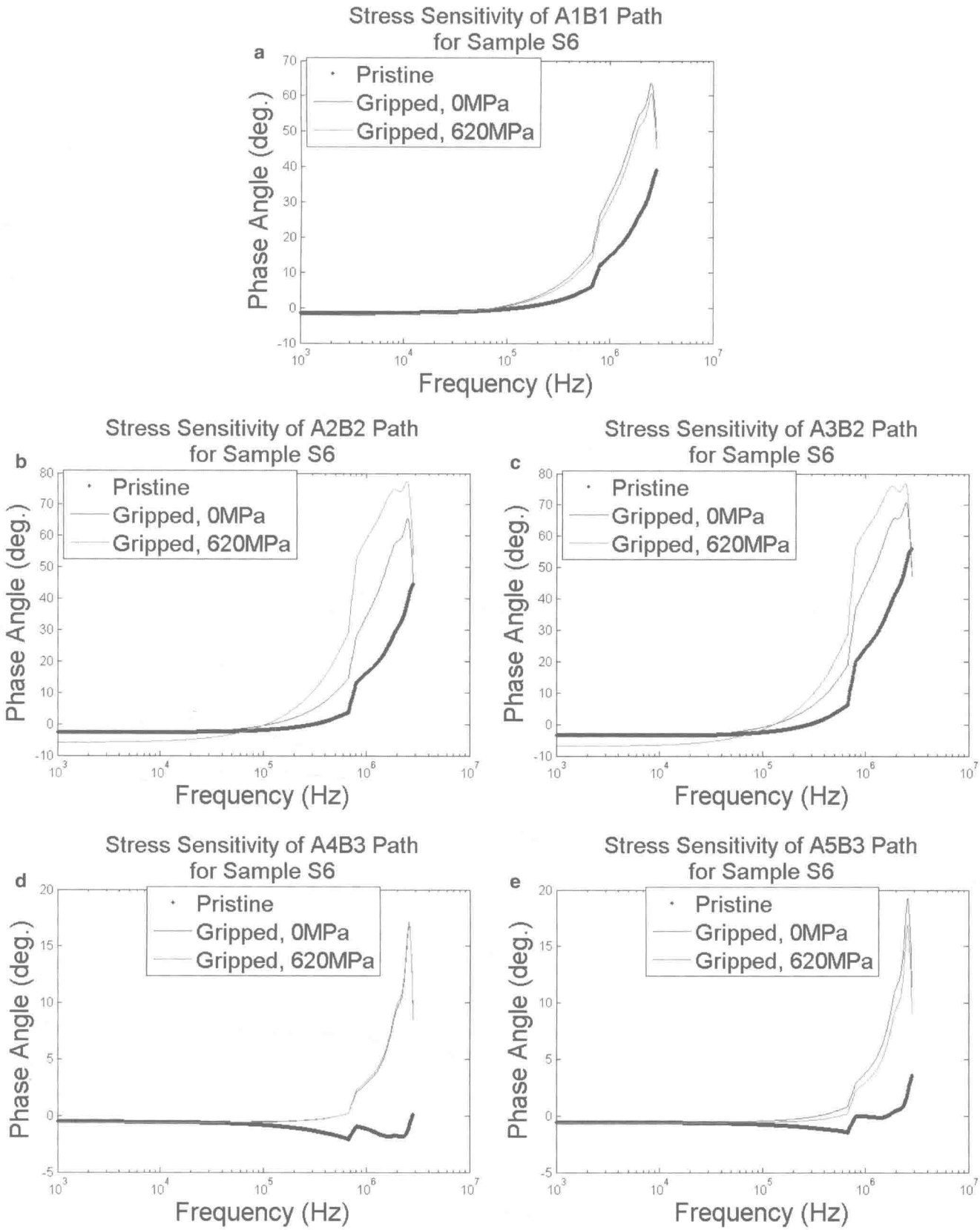

Fig. 1.5 Phase angle resolution of specimen S6 load state for different electrical paths (**a–e**)

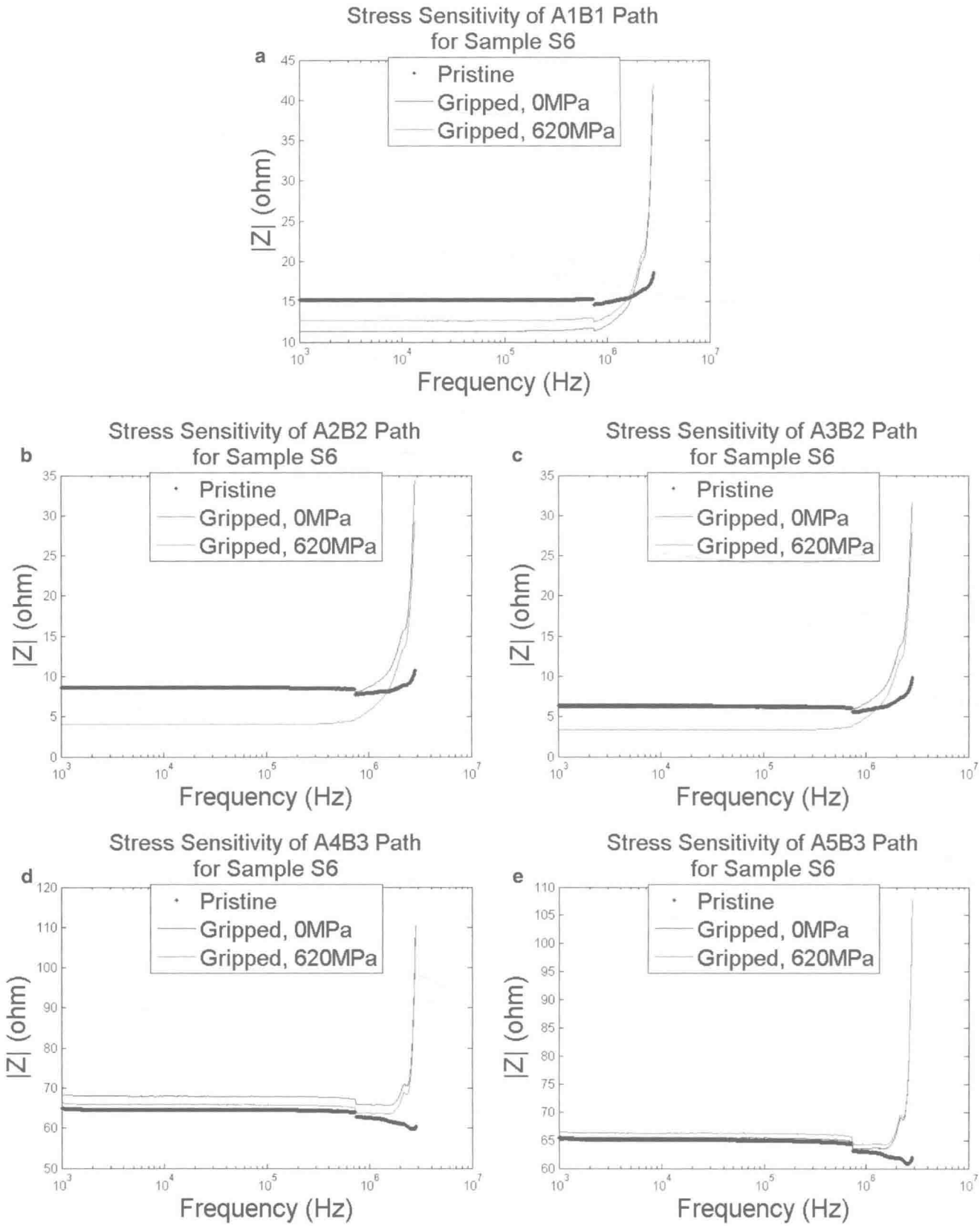

Fig. 1.6 Impedance magnitude resolution of specimen S6 load state for different electrical paths (**a–e**)

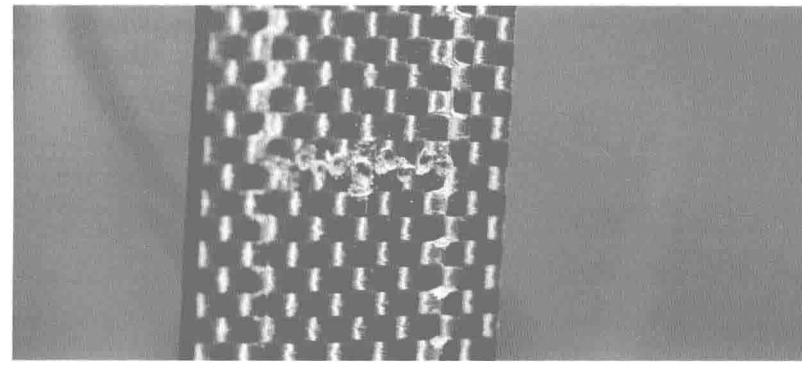

Fig. 1.7 Photograph of intentionally introduced damage to the specimen

Comparing the results from phase and impedance we conclude that phase is better at resolving sample load state at higher frequencies, whereas impedance magnitude is more sensitive at lower frequencies. For the specimens tested, the approximate cutoff frequency at which the phase becomes more effective at resolving specimen load state is about 500 kHz. Electrical path through the specimens also influences sensitivity to the load state, with paths A2B2 and A3B2 showing the highest level of sensitivity for both phase and impedance magnitude.

1.4.2 Detection of Specimen Damage State

Specimen 'S6' was scanned undamaged and unloaded. Damage was introduced to the specimen at the middle of the gage section without removing it from the grips using a spring-loaded center punch, as shown in Fig. 1.7. The specimen was then rescanned to determine if the EIS technique is capable of detecting the known presence of damage. The specimen was then subjected to 10,000 cycles at an r-ratio of 0.1 and a peak load of 50 kN to identify whether or not the EIS technique is able to detect changes in the specimen arising from a change in the damage due to the cyclic loading. All five electrical paths were interrogated using the NA at the undamaged, damaged, and damaged-cycled states. The results for phase angle can be seen in Fig. 1.8 and impedance magnitude in Fig. 1.9. The specimen damage state can be detected using both impedance magnitude and phase information from the EIS scans. The EIS technique is also capable of resolving changes in the damage state arising from the cyclic loading of the specimen. Comparing the results from phase and impedance we conclude that, as in the case with load state above, phase information is better at resolving damage state at higher frequencies, whereas impedance magnitude is more sensitive at lower frequencies. For the specimens tested, the approximate cutoff frequency at which the phase becomes more effective at resolving specimen load state is about 500 kHz, again the same result as for the load state. Electrical path through the specimens also influences sensitivity to the damage state, with paths A2B2, A3B2, and A4B3 showing the highest level of sensitivity for both phase and impedance magnitude.

1.4.3 Detection of Specimen Fatigue State

Five specimens were prepared for the fatigue testing (S1, S2, S3, S4, S5). The data for specimen S1 were inconclusive due to the aforementioned issues arising from the initial manual protocol. Samples S2 and S3 for the fatigue evaluation failed at very low numbers of cycles, and so are not included in the data presented in this paper. Therefore, the data for the fatigue sensitivity results presented in this paper are based on only two specimens, S4, and S5, and conclusions based on a sample size of two are thereby limited. Due to limitations in the way the initial experiments were performed we currently have no way to confidently discriminate between specimen fatigue damage and fatigue damage to the electrical lead bonds. Figure 1.10 shows an example of how obvious lead damage is in the phase and impedance data. Examination of the data was used to identify which leads failed, and when.

We have evidence to suggest that both types of damage are being detected. For sample S4, lead damage is apparent for the electrical path A2B2 in the impedance magnitude data shown in Fig. 1.10 at approximately 48 % cycle/failure. Similarly, lead damage was detected in S4 in electrical path A4B3 at approximately 25 % cycle/failure (see plot for S4 in Fig. 1.11). In both of these cases, the lead damage for paths A4B3 and A2B2 showed up in the scans along path A1B1 as shown in

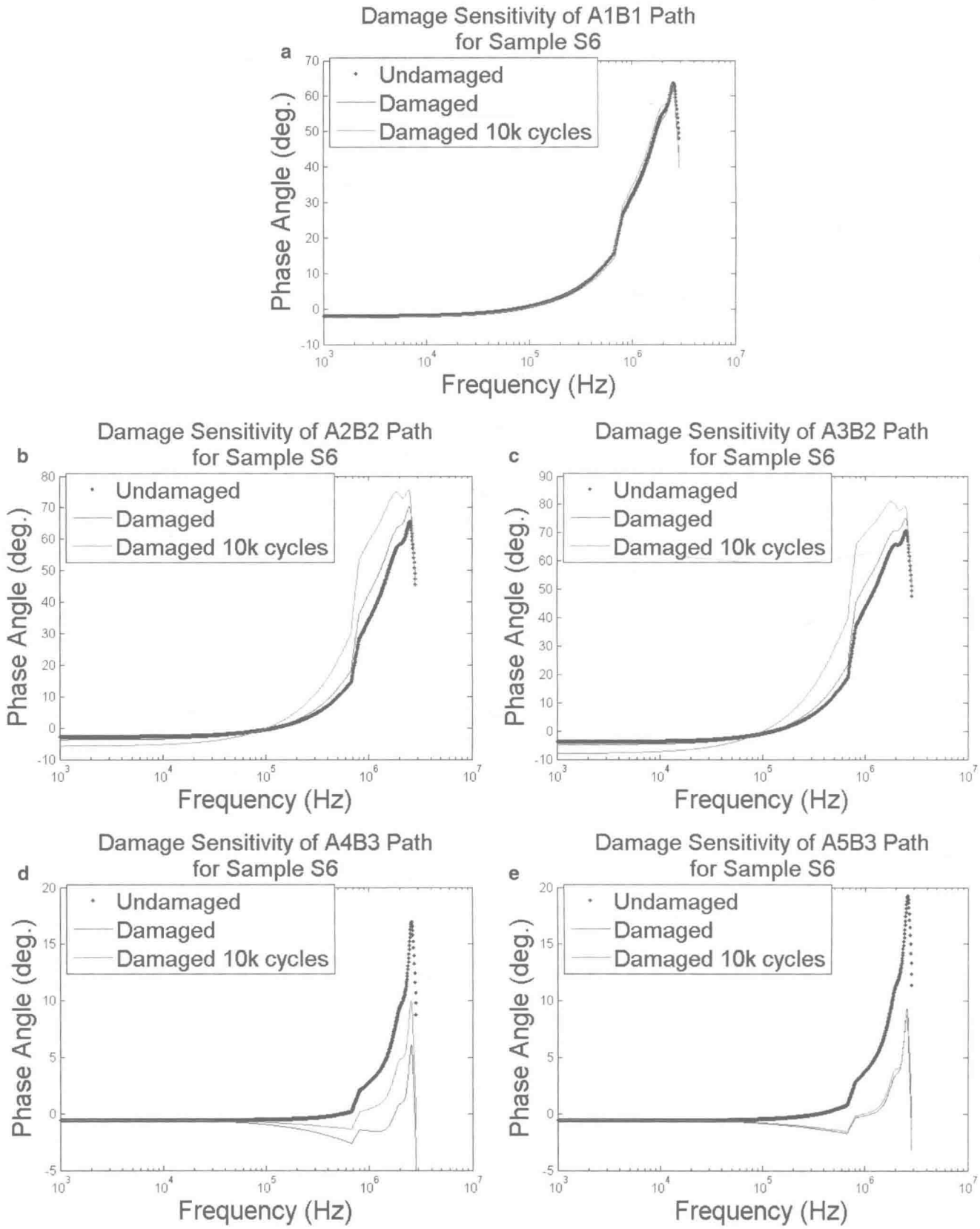

Fig. 1.8 Phase angle resolution of specimen S6 damage state for different electrical paths (**a–e**)

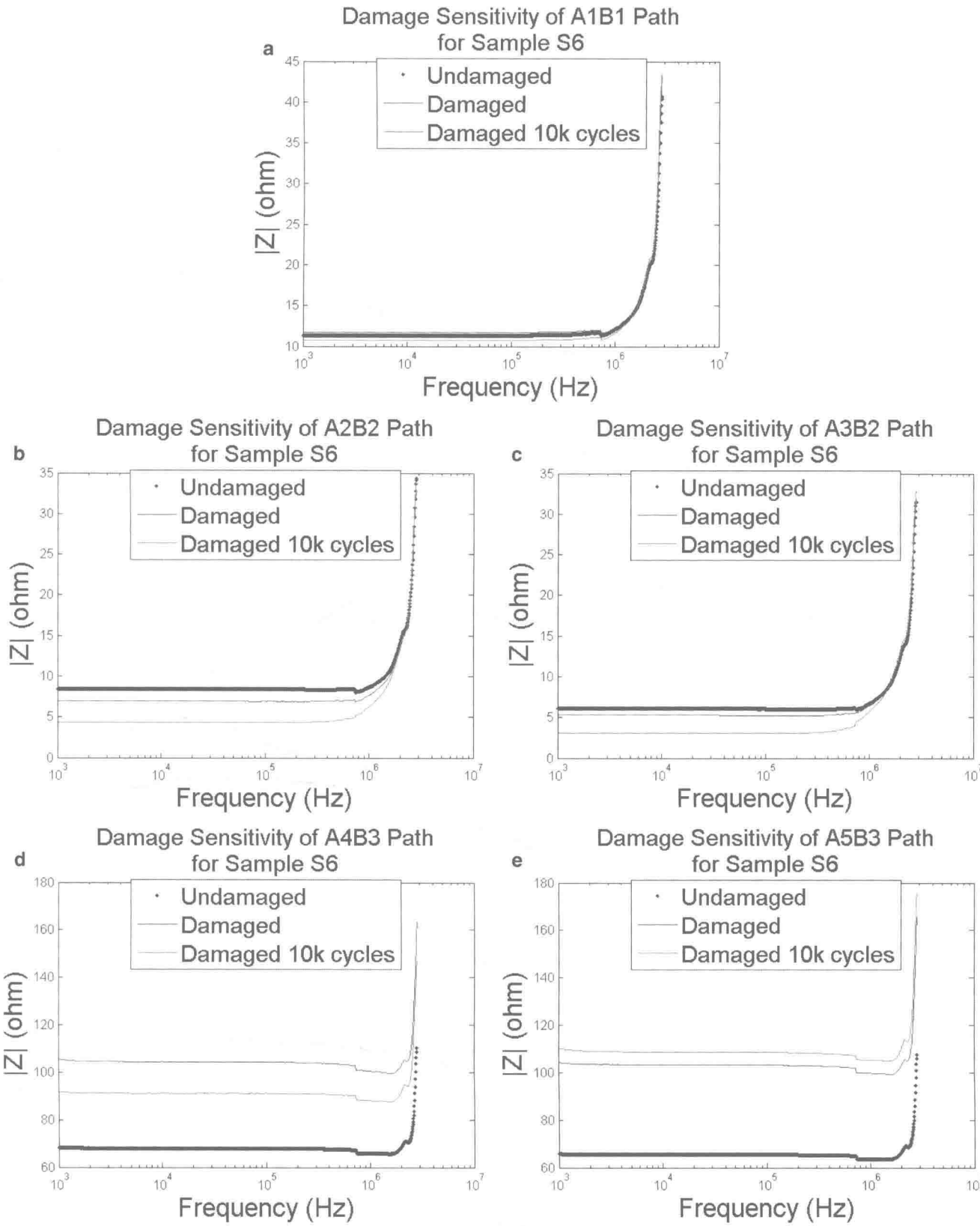

Fig. 1.9 Impedance magnitude resolution of specimen S6 damage state for different electrical paths (**a–e**)

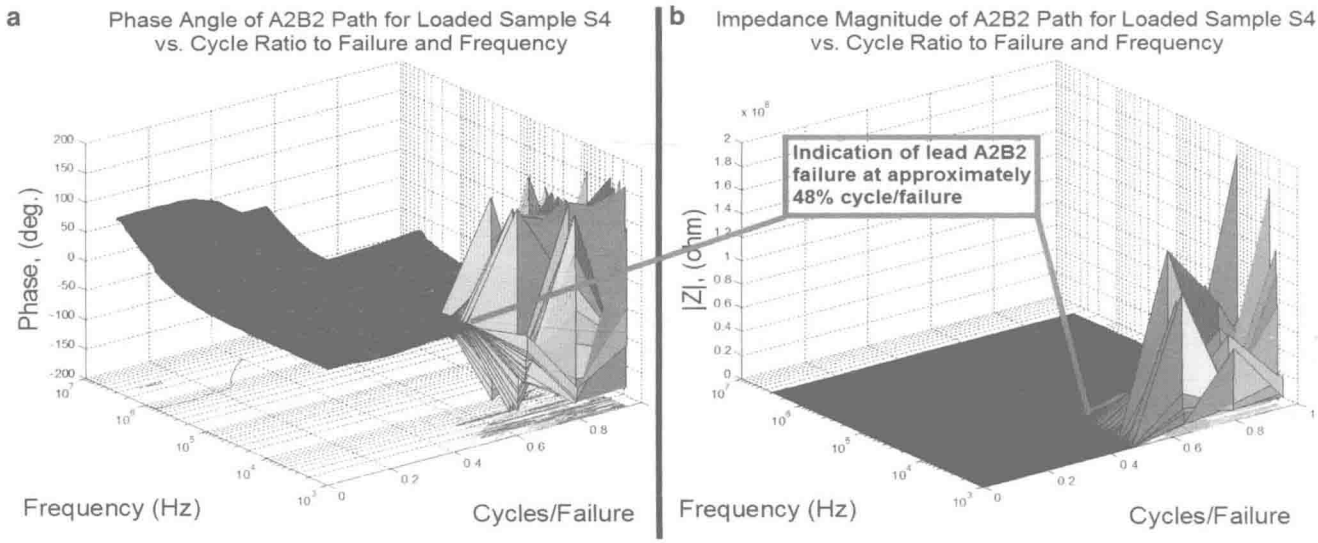

Fig. 1.10 Electrical lead failure indication in both phase angle (**a**) and impedance magnitude (**b**) data

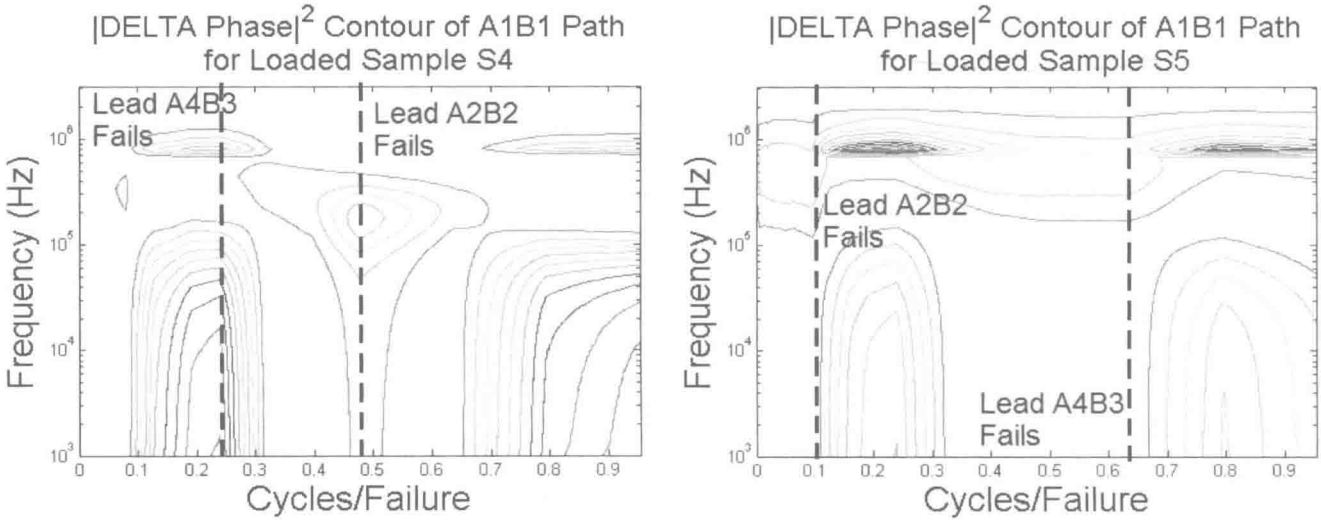

Fig. 1.11 Comparison of delta-phase contours for two specimens, S4 (*left*) and S5 (*right*), with electrical lead damage indicated in the cycle/failure domain

the left side of Fig. 1.11. Likewise, for sample 'S5,' lead damage in path A2B2 and A4B3 were detected at 10 and 62 % cycles/failure respectively, and showed up in the A1B1 electrical path scans as shown on the right side of Fig. 1.11. As also illustrated in Fig. 1.11, in the case of sample S4, the damage is correlated with the center of the contour regions, versus in sample S5, the damage is correlated with the onset (left edge) of the contour regions.

Lead damage is not correlated with the contour region at the right side of the S4 scan in Fig. 1.11, thus leading us to believe that this region may be indicative of damage manifesting in the sample itself, and leading to eventual specimen failure. We need to further refine our experimental techniques to allow for reliable and confident discrimination between specimen damage and damage to the electrical leads. We have multiple strategies to realize this: (1) remove the electrical leads from the gage length of the specimens to the extent possible in order to eliminate the potential for electrical lead damage; (2) analyze specimens with single pairs of electrical leads to eliminate the possibility of electrical paths into/out of the specimens via the passive non-scanning leads.